Partial Characterization of the Sox2+ Cell Population in an Adult Murine Model of Digit Amputation

Vineet Agrawal, Ph.D.,[1,2] Bernard F. Siu, B.S.E.,[1,3,*] Hsu Chao, Ph.D.,[4,*] Karen K. Hirschi, Ph.D.,[4] Eric Raborn, B.S.E.,[4] Scott A. Johnson, M.S.,[1,5] Stephen Tottey, Ph.D.,[1,5] Katherine B. Hurley, B.S.,[1] Chris J. Medberry, B.S.,[1,3] and Stephen F. Badylak, D.V.M., M.D., Ph.D.[1,3,5]

Tissue regeneration in response to injury in adult mammals is generally limited to select tissues. Nonmammalian species such as newts and axolotls undergo regeneration of complex tissues such as limbs and digits via recruitment and accumulation of local and circulating multipotent progenitors preprogrammed to recapitulate the missing tissue. Directed recruitment and activation of progenitor cells at a site of injury in adult mammals may alter the default wound-healing response from scar tissue toward regeneration. Bioactive molecules derived from proteolytic degradation of extracellular matrix (ECM) proteins have been shown to recruit a variety of progenitor cells *in vitro* and *in vivo* to the site of injury. The present study further characterized the population of cells accumulating at the site of injury after treatment with ECM degradation products in a well-established model of murine digit amputation. After a mid-second phalanx digit amputation in 6–8-week-old adult mice, treatment with ECM degradation products resulted in the accumulation of a heterogeneous population of cells, a subset of which expressed the transcription factor Sox2, a marker of pluripotent and adult progenitor cells. Sox2+ cells were localized lateral to the amputated P2 bone and coexpressed progenitor cell markers CD90 and Sca1. Transgenic Sox2 *eGFP/+* and bone marrow chimeric mice showed that the bone marrow and blood circulation did not contribute to the Sox2+ cell population. The present study showed that, in addition to circulating progenitor cells, resident tissue-derived cells also populate at the site of injury after treatment with ECM degradation products. Although future work is necessary to determine the contribution of Sox2+ cells to functional tissue at the site of injury, recruitment and/or activation of local tissue-derived cells may be a viable approach to tissue engineering of more complex tissues in adult mammals.

Introduction

Tissue regeneration in response to injury is limited in adult mammals, with the default response to injury, generally involving rapid infiltration of inflammatory cells and eventual scar tissue deposition. Nonmammalian species such as newts and axolotls are capable of regeneration of complex tissues such as limbs and digits through a process known as blastemal-based epimorphic regeneration, in which soluble factors and specific genetic programs are activated to recruit a population of multipotent stem cells preprogrammed to recapitulate a perfect phenocopy of the missing tissue.[1–3] While a blastema does not form after injury in adult mammalian species, recruitment to and/or directed differentiation of tissue-specific progenitor cells at the site of injury has the potential to alter the default wound-healing response toward nonblastemal, epimorphic regeneration.[4,5]

Biological scaffolds composed of extracellular matrix (ECM) have been used to promote site-specific, functional remodeling of tissue in both preclinical animal models[6–13] and human clinical applications.[14–18] Although the mechanisms underlying remodeling are not completely understood, the release of bioactive peptides after ECM scaffold degradation and concomitant accumulation of progenitor cells at the site of injury are thought to be two important mechanisms by which ECM scaffolds promote constructive tissue remodeling of the injury site.[19–22] Specifically, previous studies have shown that circulating and bone marrow-derived progenitor cells partially comprise the population of cells that infiltrate at the site of ECM implantation[23,24] and eventually contribute to site-appropriate differentiated and remodeled tissue.[19,20]

One possible mechanism by which progenitor cells are recruited to the site of injury is via the release of chemotactic

---

[1]McGowan Institute for Regenerative Medicine, University of Pittsburgh, Pittsburgh, Pennsylvania.
[2]Medical Scientist Training Program, University of Pittsburgh, Pittsburgh, Pennylvania.
[3]Department of Bioengineering, University of Pittsburgh, Pittsburgh, Pennylvania.
[4]Department of Internal Medicine, Yale Cardiovascular Research Center, Yale University School of Medicine, New Haven, Connecticut.
[5]Department of Surgery, University of Pittsburgh, Pittsburgh, Pennsylvania.
*These two authors contributed equally to this work.

cryptic peptides. Peptides derived from degradation of ECM scaffolds have been shown to have potent chemotactic and mitogenic properties for multiple progenitor cells *in vitro*.[25–27] Additionally, treatment with these ECM degradation products results in the accumulation of cells with multipotent lineage differentiation potential in an adult mammalian model of digit amputation.[21] A subset of these cells expresses the transcription factor Sox2,[21,28,29] a factor that plays an important role in self-renewal of stem cells, including neural, dermal, neural crest–derived, and osteogenic progenitor cells.[30–33] However, the phenotype and role of Sox2+ cells at the site of digit amputation have not yet been investigated.

The present study partially characterizes the source and phenotype of the Sox2+ population of cells that is recruited in response to treatment with matrix degradation products in an established adult mammalian model of mid-second phalanx digit amputation.

Materials and Methods

General overview

All methods were approved by the Institutional Animal Care and Use Committees (IACUC) at the University of Pittsburgh and Baylor College of Medicine, and all methods were performed in compliance with NIH Guidelines for the Care and Use of Laboratory Animals. The studies were designed to further characterize the phenotype and source of a previously identified population of progenitor cells that accumulate at the site of injury after digit amputation in adult mice.[21,29] Histologic analysis and flow cytometric analysis were used to characterize the heterogeneity, density, and phenotype of the accumulated cells after treatment with ECM degradation products. Additionally, a bone marrow chimeric mouse model was utilized to investigate the contribution of the bone marrow-derived cells to the Sox2+ population of cells at the site of amputation.

Preparation of ECM degradation products

The basement membrane and underlying lamina propria of market-weight porcine urinary bladders were isolated and harvested as previously described.[34] After peracetic acid, deionized H_2O, and phosphate-buffered saline treatment,[25] lyophilized sheets were comminuted and digested in pepsin and 0.01 N HCl for 48 h before neutralization and dilution in phosphate-buffered saline (PBS) to yield a 5 mg/mL solution (referred to as ECM degradation products).

Fluorescein isothiocyanate labeling of ECM degradation products

To confirm that ECM degradation products injected at the base of the amputated foot reach the site of amputation, degradation products of ECM were labeled with the fluorescein isothiocyanate (FITC) fluorophore as per manufacturer's instructions (Thermo PierceNet; #53027). After mid-second phalanx amputation under isoflurane anesthesia, FITC-labeled ECM degradation products were injected at the base of the amputated digit. After injection, animals were immediately sacrificed, and the entire foot was isolated and fixed in 4% paraformaldehyde before serial dehydration in 25%, 50%, 75%, 95%, and 100% acetone. After dehydration, fixed digits were then incubated in the Dent's fixative (1:4

dimethyl sulfoxide [DMSO]:acetone) for 2 h. Then, the digits were permeablized and bleached overnight in Dent's bleach (1:4:1 DMSO:acetone:H_2O_2). Digits were then equilibrated to a clearing solution consisting of 1:2 benzyl alcohol (Sigma; 402834) to benzyl benzoate (Sigma; B6630) (BABB) by serial 1-h incubations in 1:3, 1:1, and 3:1 solutions of BABB:Dent's fixative. Afterward, digits were then kept in 100% BABB until they were visibly optically cleared. Optically cleared digits were then imaged using a Nikon E600 epifluorescent microscope at 100× magnification, and images were taken with a Nuance camera. Images were deconvolved with a known FITC and tissue autofluorescence spectra and false colored as green and red, respectively. FITC-labeled ECM degradation products were found at the site of injection and tracking along multiple digits, including the amputated digit.

Animal model of digit amputation

Digit amputation and treatment with ECM degradation products were completed as previously described.[21] Briefly, 6–8-week-old adult C57/BL6 mice (Jackson Laboratories) were subjected to aseptic mid-second phalanx amputation of the third digit bilaterally. On days 0, 1, and 4 postamputation, 15 μL of either ECM degradation products or control injection (sham injection or PBS) was injected at the base of each amputated digit. Animals were euthanized at various time points for histologic analysis and immunolabeling, or for isolation and further analysis of cells by flow cytometric and cytospin methods. ($n=4$ for each time point and treatment group.)

Joint amputation

To determine the effect of bone injury upon cell recruitment, animals were divided into three groups. In the first group, mice were subjected to mid-second phalanx digit amputation and no treatment. In the second group, mice were subjected to mid-second phalanx digit amputation and treatment with ECM degradation products (as described above). In the third group, mice were amputated proximal to the second phalanx in the joint space to avoid any bone injury and treated with ECM degradation products. At 14 days postamputation and treatment, animals were euthanized, and digits were harvested for histologic analysis and immunolabeling. ($n=4$ for each treatment group.)

Cell isolation

Cells were isolated as previously described.[21] Briefly, digits were harvested on day 14 postamputation and placed in a cold culture medium consisting of Dulbecco's Modified Eagle's Medium (DMEM), 10% fetal bovine serum (Hyclone), 100 U/mL penicillin, and 100 μg/mL streptomycin (Invitrogen). Under a microdissection microscope, the overlying epidermal and dermal tissue was removed, and all tissue distal to the amputated bone was harvested in to the serum-free DMEM containing 0.2% Collagenase Type II (Gibco Invitrogen; 17101–015) for 30 min at 37°C. Cells were then centrifuged and reconstituted into a warm culture medium, filtered through a 70-μm filter, and counted on a hemocytometer before either cytopsin or further immunolabeling for the flow cytometric analysis.

Flow cytometric analysis

After isolation of cells, cells were spun and resuspended in 200 μL in the serum-free DMEM before incubation with primary antibodies for 1 h at 4°C. Primary antibodies were FITC-Sca1 (clone D7) (Abcam; ab25031), PE-CD133 (clone 13A4) (eBiosciences; 12–1331), e450NC-CD90.2 (clone 53–2.1) (eBiosciences; 48–0902), biotin-cKit (clone 2B8) (eBiosciences; 13–1171), and SAv-APC-Cy7 (BD Biosciences; 554063). Primary antibodies were incubated at a dilution of 1:200, and streptavidin conjugates were incubated at a dilution of 1:250 after washing away the primary antibody. Cells were then fixed and labeled for APC-Sox2 by following the manufacturer's guidelines in the BD Mouse Pluripotent Stem Cell Transcription Factor Analysis Kit (BD Biosciences; 560585). Cells were extensively washed, resuspended in PBS, and filtered through a 70-μm filter before the flow cytometric analysis.

Immunolabeling of histologic sections

Harvested mouse digits were fixed in 10% neutral buffered formalin and decalcified for 2 weeks in 5% formic acid before being paraffin embedded, sectioned, and stained for Sox2 (Millipore; AB5603). After deparaffinization, the antigen was retrieved in 10 mM citrate buffer (C1285; Spectrum) for 25 min at 95°C–100°C. Slides were blocked for 1 h at room temperature in 1% bovine serum albumin (BSA) in PBS, and then incubated with the primary antibody overnight at 4°C. Slides were then rinsed in PBS, treated with a 3% hydrogen peroxide solution in PBS for 30 min, washed, and incubated for 1 h with horseradish peroxidase–conjugated anti-rat IgG (P0450; Dako) or anti-rabbit IgG (P0448; Dako) antibodies, washed, and developed with 3, 3' diaminobenzidine (DAB) (Vector Labs). All primary antibodies were diluted 1:100 in a blocking solution, and all secondary antibodies were diluted 1:200 in a blocking solution. After staining with DAB, all slides were counterstained with Harris' hematoxylin, dehydrated, coverslipped with a nonaqueous mounting medium, and imaged at a $320\times$ magnification. For quantification of the number of cells positive for markers, three images were taken in each sample: distal to the amputated edge of the second phalanx bone, and lateral to the cut edge of the second phalanx bone on either side. The number of positive cells in each image was counted by three independent investigators who were blinded to the treatment group.

Immunolabeling of cytospin samples

After cytospin of 1×10^4 isolated cells per slide, each slide was fixed in methanol for 30 s and stored at -20°C. Before staining, slides were rehydrated in PBS for 5 min, and cells were permeablized in 0.1% Triton X/PBS for 15 min. Slides were blocked in 1% bovine serum albumin/PBS for 1 h before overnight incubation with rabbit anti-Sox2 (1:100) and/or chicken anti-GFP (1:100) (Abcam; ab13970) diluted in a blocking solution. After two washes in PBS, slides were incubated for 1 h with donkey anti-rabbit IgG-Alexa Fluor 488 (1:250) (Invitrogen; A21206), donkey anti-rabbit IgG-Alexa Fluor 546 (1:250) (Invitrogen; A10040), and/or donkey anti-chicken IgG-Alexa Fluor 488 (1:250) (Invitrogen; A11039) diluted in a blocking solution. After two washes in PBS, slides were counterstained with DRAQ5 (1:500) (Cell Signal; 4084) diluted in PBS for 30 s before three washes in PBS and

coverslipping with a fluorescent mounting medium (Dako; S3023). All images were taken at $200\times$ magnification.

Whole-bone marrow cell isolation, bone marrow transplantation, and engraftment analysis

For every animal, bone marrow was isolated from tibias and femurs. The bones were dissected and crushed in a mortar and pestle in a cold Hanks Balanced Salt Solution (Invitrogen) containing 2% FCS, 2% fetal bovine serum (Invitrogen), and 10 mM HEPES (Invitrogen). The cells were passed through a 40-mm filter to ensure single-cell suspension. Red blood cells (RBCs) were lyzed in 9 mL of water followed by adding 1 mL of $10\times$PBS. Cells were washed twice in $1\times$PBS and suspended in PBS at 1×10^8/mL. 1×10^6 Sox2:enhanced green fluorescent protein (EGFP) (CD45.2) bone marrow cells were transplanted into lethally irradiated (10.5 Gy) CD45.1 wild-type recipient mice by tail vein injection. Long-term bone marrow engraftment by Sox2:EGFP donor bone marrow HSCs was measured by peripheral blood contribution at 12-week post-transplantation. Briefly, 200 μL peripheral blood was collected from the retro-orbital plexus of anesthetized transplant recipients. RBCs were lyzed and washed. Nucleated cells were then stained with both CD45.1 and CD45.2 antibodies. Stained blood samples were then analyzed by flow cytometry using FACSaria (BD Biosciences).

Isolation and analysis of subventricular zone cells from Sox2 eGFP/+ mice

Sox2+ cells were isolated from the subventricular zone (SVZ) of the brains of Sox2 *eGFP*/+ mice using a modified version of a previously reported protocol.[35] The SVZ was removed using curved microscissors (Roboz) to minimize striatal tissue inclusion in the sample. The isolated tissue was cut into small pieces and resuspended in DMEM/F12 (Invitrogen) with activated papain (Worthington) at 10 U/mL and DNase (Roche) at 10 U/mL. The tissue was incubated at 37°C for 45 min in a rolling incubator to allow for constant mixing. At 30 min, the tissue was triturated with a 5-mL pipette ∼10 times before being returned to the rolling incubator. At 45 min, the tissue suspension was collected via centrifugation and resuspended in DMEM/F12 with 0.7 g/mL of ovomucoid (Sigma-Aldrich) and 10 U/mL DNase. The solution was triturated again with a 5-mL pipette until no aggregations were visible with the naked eye before passing the solution through a 40-μm strainer to remove debris and cell aggregates. The SVZ of the adult mouse brain was used as a positive control for the Sox2/*eGFP*+ reporter, because the neural lineage cell populations comprising the niche all express Sox2.[36,37]

Results

ECM degradation products reach the site of amputation

To directly assess whether ECM degradation products injected at the base of an amputated digit reach the site of amputation, ECM degradation products were nonspecifically covalently attached to an FITC fluorophore. The labeled ECM degradation product injectate was found to diffuse into the amputated digit as well as into adjacent, unamputated digits (Fig. 1). Labeled ECM degradation products were not
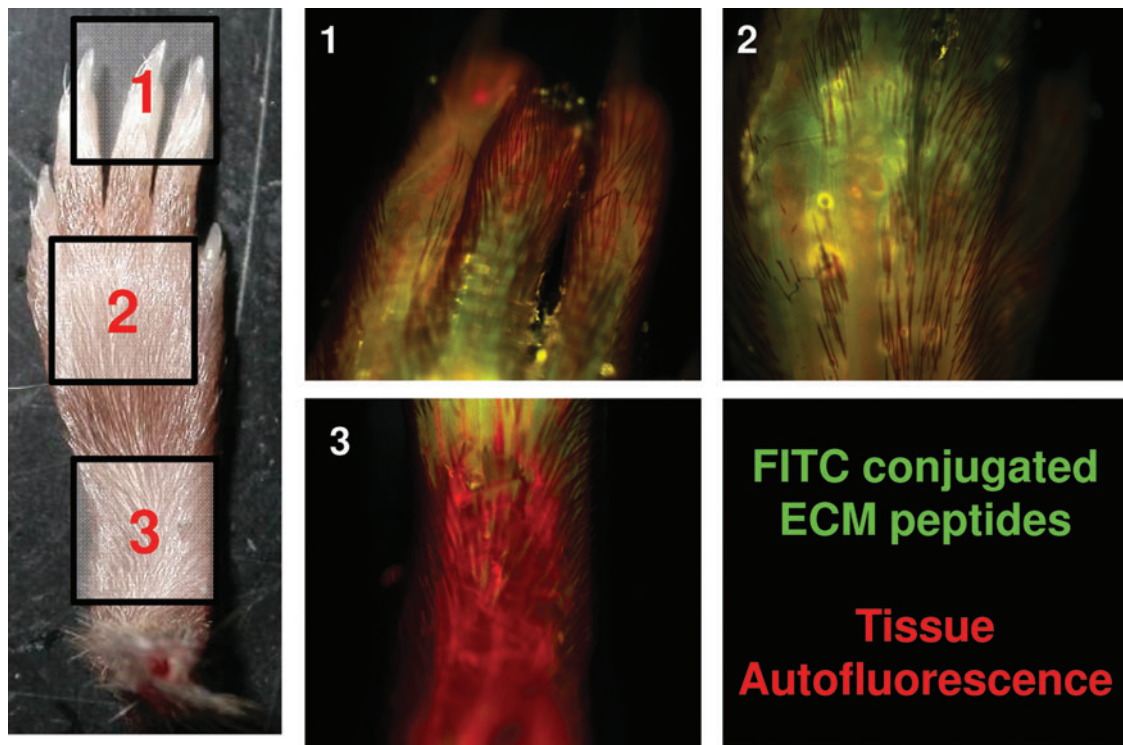
FIG. 1. Extracellular matrix (ECM) degradation products reach the site of amputation. After injecting fluorescein iso-thiocyanate-conjugated ECM degradation products at the base of the amputated digit, ECM degradation products were found diffusing along the amputated digit as well as adjacent unamputated digits. Color images available online at www .liebertpub.com/tea
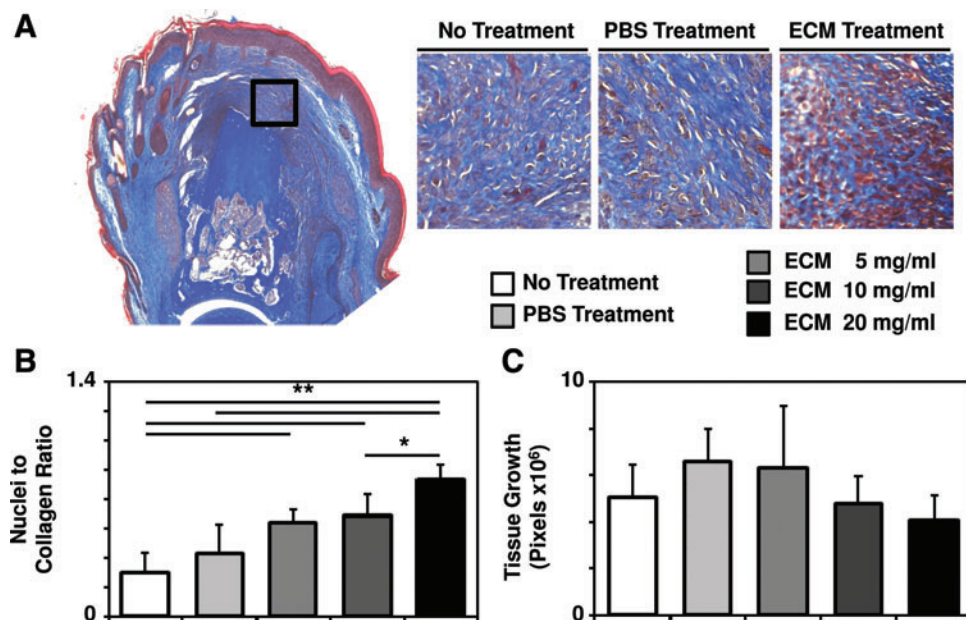

FIG. 2. ECM treatment causes a more densely cellular accumulation at the site of digit amputation. **(A)** After mid-second phalanx digit amputation and treatment with ECM degradation products or control, histologic analysis of Trichrome-stained sections at day 14 postamputation showed the appearance of a more densely cellular accumulation at the site of amputation after ECM treatment. **(B)** This was confirmed by automated quantification of the relative ratio of cellularity to connective tissue of the Trichrome stain. **(C)** Quantification of the area of growth distal to the site of amputation showed no difference between ECM treatment and no treatment. $*p < 0.05$ and $**p < 0.01$.; Error bars are mean$\pm$SD ($n = 4$ for each group). Color images available online at www.liebertpub.com/tea
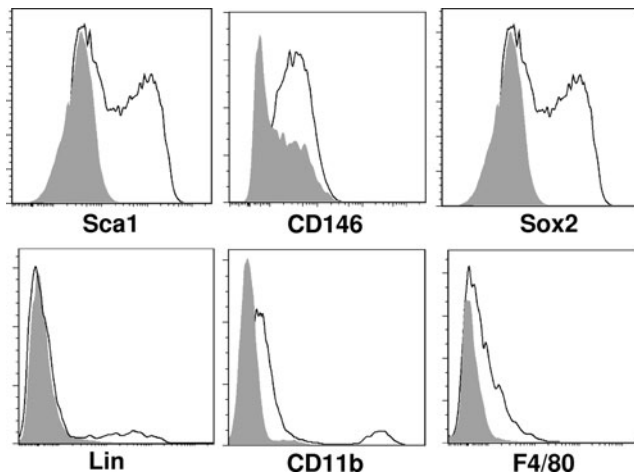
FIG. 3. ECM treatment results in the accumulation of a heterogeneous population of cells at the site of amputation. After digit amputation and treatment with either ECM degradation products or control, the accumulation of cells at the site of amputation (Fig. 2.) was microdissected and dissociated for further analysis. Flow cytometric analysis showed that subsets of cells expressed markers Sca1, CD146, Sox2, Lineage, CD11b, and F4/80.

used for any further studies because of the known profibrotic effect of FITC *in vivo.*[38]

ECM treatment results in an increased density of cells at the site of amputation

At day 14 postamputation, treatment with ECM degradation products led to a dense accumulation of cells at the site of amputation, whereas no treatment resulted in a less cellular accumulation concomitant with scar tissue deposi-

tion at the site of amputation, consistent with a completed wound-healing response to murine digit amputation (Fig. 2A).[39,40] Histologic appearance of an increased cell density after ECM treatment was confirmed by quantification of the relative ratio of cellularity to connective tissue on Trichrome slides (Fig. 2B and Supplementary Fig. S1; Supplementary Data are available online at www.liebertpub.com/tea). Quantification of the total area of growth distal to the site of amputation showed no difference between ECM treatment and no treatment, suggesting that the accumulated cells were more densely populated within the newly formed tissue area after ECM treatment (Fig. 2C, Supplementary Fig. S2).

ECM treatment leads to heterogeneous accumulation of cells at the site of amputation

To further characterize the accumulated cells at the site of amputation, the area of new tissue growth was microdissected and dissociated for the flow cytometric analysis. Flow cytometric analysis of the isolated cells confirmed a heterogeneous population with subsets of cells that express progenitor cell markers such as Sca1, Sox2, and CD146 as well as subsets that express differentiated macrophage markers, including CD11b and F4/80 (Fig. 3).

ECM treatment results in Sox2+ cell accumulation at the site of amputation

After treatment with ECM degradation products, a greater number of Sox2+ cells were present at the site of amputation at days 10, 14, and 18 postamputation as compared to digits treated with PBS (Fig. 4A and Supplementary Fig. S3). Expression of Sox2+ cells was confirmed by both immunolabeling of cytospin slides (Fig. 4B) and flow cytometry (Fig. 4C). Sox2 expression was predominantly localized to the cytoplasm of cells, with a subset of cells showing nuclear and cytoplasmic localization. Flow cytometric analysis showed that the Sox2+
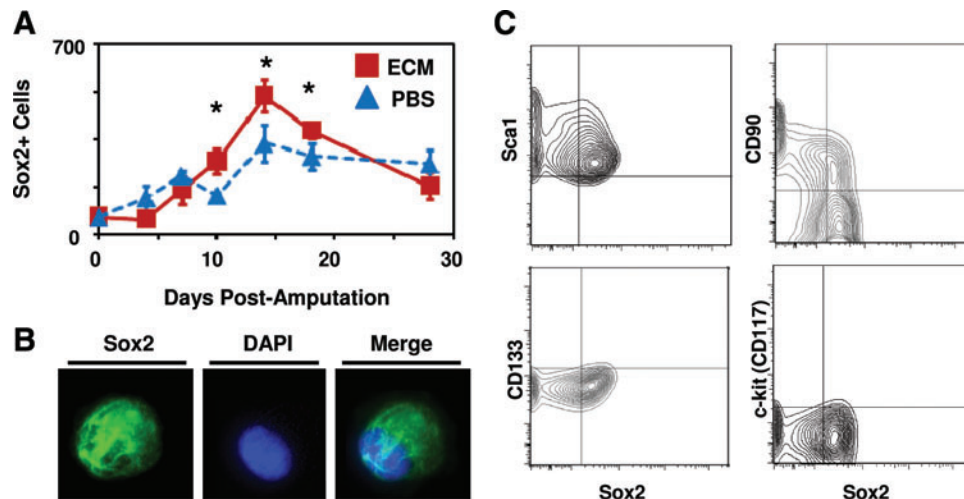

FIG. 4. ECM treatment results in a greater number of Sox2+ cells at the site of amputation. **(A)** After digit amputation and treatment with ECM degradation products or control, digits were fixed at various time points postamputation, sectioned for histologic analysis, and immunolabeled for the presence of Sox2. A greater number of Sox2+ cells were observed at the site of amputation on days 10, 14, and 18 postamputation. **(B)** After microdissection and dissociation of the cell accumulation at the site of amputation, Sox2+ cell expression was confirmed by immunolabeling of cells cytospun on to a slide. **(C)** Flow cytometric analysis of the isolated cells showed that Sox2+ cells coexpressed Sca1 and CD90, but not CD133 or c-kit. *$p < 0.05$. Error bars are mean $\pm$ SEM ($n = 4$ for each group). Color images available online at www.liebertpub.com/tea
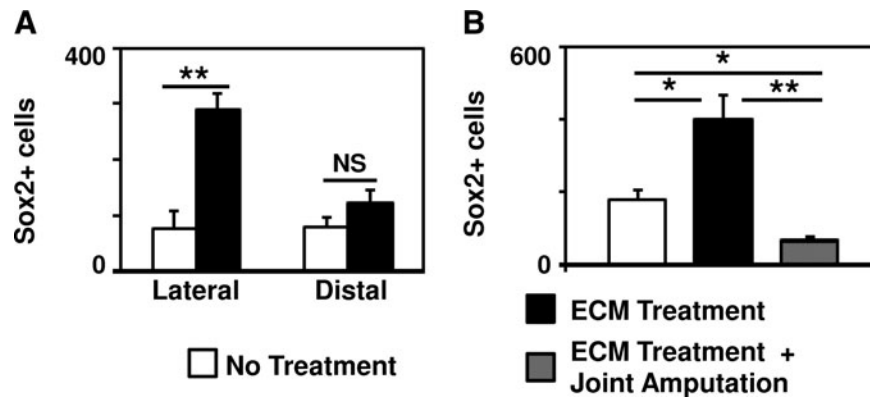
FIG. 5. Sox2+ cell accumulation requires bone injury and is located lateral to the amputated bone. **(A)** Immunolabeling of histologic sections of amputated digits showed that the majority of Sox2+ cells present at the site of amputation after treatment with ECM degradation products were located lateral to the amputated P2 bone, consistent with a periosteal location. **(B)** After digit amputation proximal to P2 bone at the joint such that no bone injury was induced, the accumulation of Sox2+ cells at the site of amputation after ECM degradation products was decreased. $*p < 0.05$. $**p < 0.01$. Error bars are mean ± SEM ($n = 4$ for each group).

cells did not express progenitor cell markers CD133[33] or c-kit,[41,42] but did coexpress Sca1 and CD90, known markers of bone marrow and periosteal mesenchymal stem cells[43,44] (Fig. 4C). Immunolabeling of histologic sections of amputated digits showed that the majority of Sox2+ cells were present lateral to the amputated bone, along the external surface of the cortex of the bone (Fig. 5A and Supplementary Fig. S3). After amputation at the proximal interphalangeal joint in which only soft tissue injury, but no bone injury was induced, the accumulation of Sox2+ cells was markedly reduced (Fig. 5B).

Sox2+ cells are not derived from the bone marrow

To determine the contribution of bone marrow-derived Sox2+ cells to the cell accumulation at the site of amputation, the bone marrow of Sox2/eGFP+ mice (expressing the CD45.2 antigen) was transplanted into genetically and age-matched C57/BL6 mice (expressing the CD45.1 antigen).
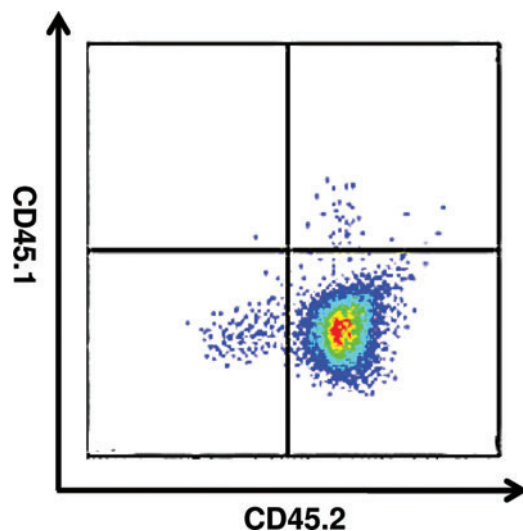

FIG. 6. Confirmation of stable engraftment of bone marrow transplanted mice. To confirm stable engraftment of Sox2 eGFP/+ bone marrow transplanted into adult wild type C57/BL6 mice, blood from transplanted mice was analyzed at 4 weeks postengraftment for expression of CD45.2 (Sox2 eGFP/+) and CD45.1 (wild type). At 4 weeks postengraftment, the blood of mice expressed the CD45.2 on blood-derived cells, confirming stable engraftment of Sox2/eGFP+ bone marrow in mice. Color images available online at www.liebertpub.com/tea
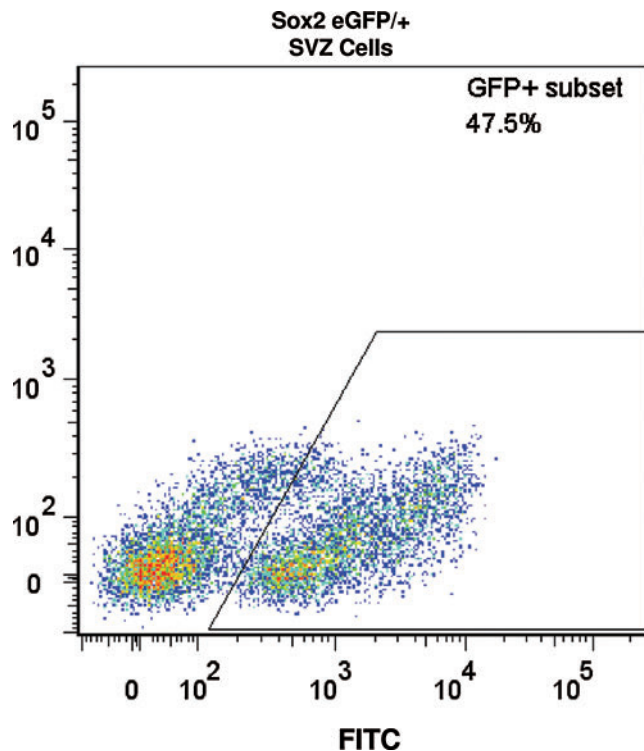

FIG. 7. Confirmation of eGFP+ expression in Sox2+ cells from the subventricular zone (SVZ) of adult Sox2 eGFP/+ mice. Cells from the SVZ of the adult brain of Sox2 eGFP/+ mice were isolated to confirm eGFP+ expression. GFP+ expression was confirmed in a subset of the SVZ, as previously shown.[35–37] Isolated bone marrows did not express eGFP. Color images available online at www.liebertpub.com/tea
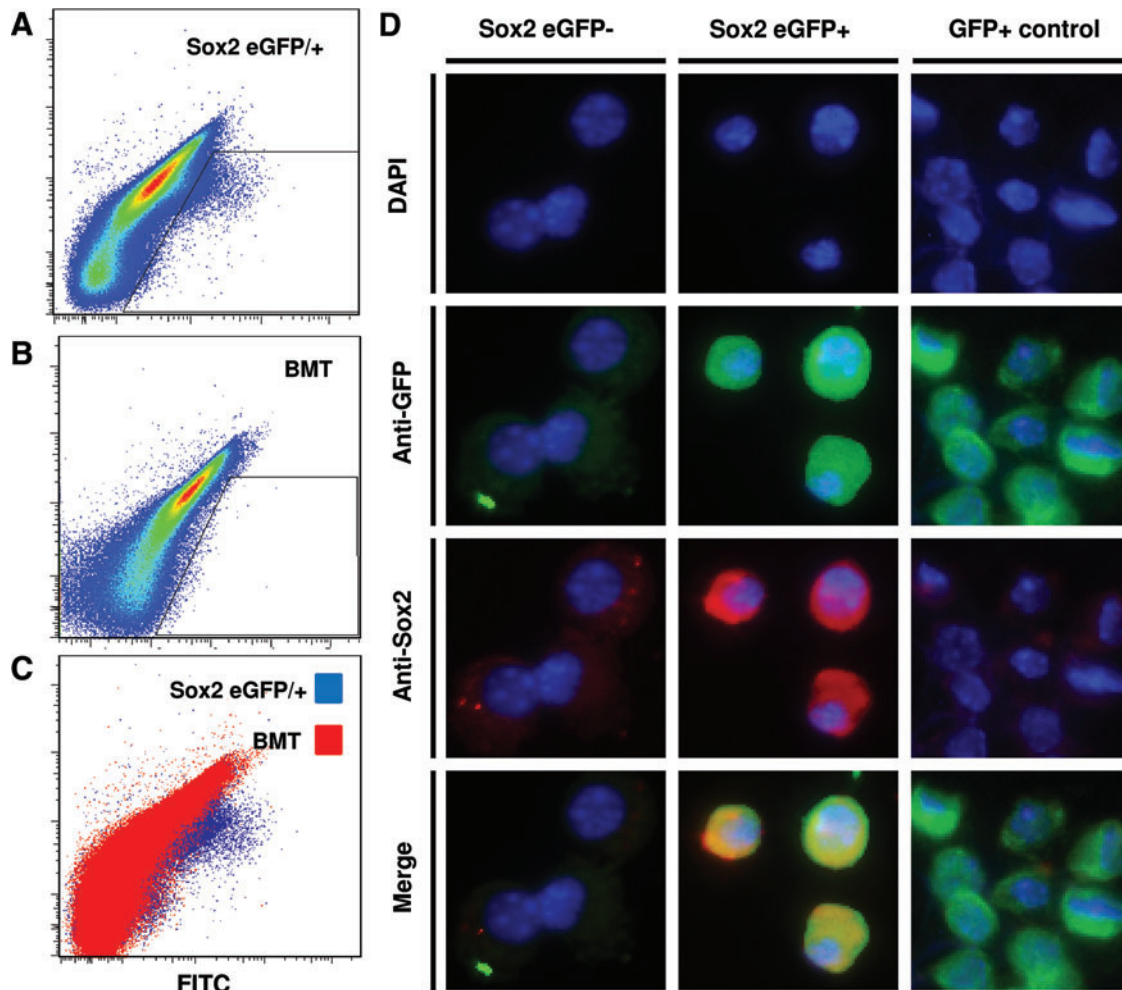
FIG. 8. Sox2 + cells at the site of digit amputation are not derived from the bone marrow or circulation. Sox2 *eGFP* / + transgenic mice and genetically matched, wild-type C57/BL6 transplanted with Sox2 *eGFP* / + bone marrow were subjected to mid-second phalanx digit amputation and treatment with ECM degradation products. At day 14 postamputation, cells at the site of amputation were microdissected and dissociated for flow cytometric analysis for GFP expression. **(A)** GFP + cells were found in cells isolated from Sox2 *eGFP* / + transgenic mice. **(B)** A GFP + population of cells was not found in cells isolated from bone marrow chimeric wild-type mice. **(C)** Cells isolated from Sox2 *eGFP* / + mice showed a population of cells by flow cytometric analysis that was not present in bone marrow chimeric wild-type mice. **(D)** After sorting and cytospinning GFP + and GFP− cell populations, immunolabeling confirmed that the GFP + cells expressed Sox2 and GFP, whereas GFP− cells did not express Sox2 or GFP. Color images available online at www.liebertpub.com/tea

Bone marrow chimeric mice all displayed stable engraftment 4 weeks post-transplant with, confirmed by the presence of CD45.2 +, CD45.1− blood cells (Fig. 6). To confirm *eGFP* + expression in donor mice, known Sox2 + SVZ cells were isolated from donor mice and analyzed by flow cytometry to confirm GFP + expression (Fig. 7). Both Sox2 *eGFP* / + mice and wild-type mice transplanted with Sox2 *eGFP* / + bone marrow were subjected to mid-second phalanx digit amputation bilaterally and treatment with ECM degradation products. On day 14 postamputation, cells were microdissected and isolated from digits of Sox2 *eGFP* / + transgenic mice as well as bone marrow chimeric mice. The flow cytometric analysis confirmed *eGFP* + cells at the site of amputation in Sox2 *eGFP* / + mice (Fig. 8A), but no *eGFP* + cells from amputated digits of bone marrow chimeric mice (Fig. 8B, C). *eGFP* + and *eGFP* − populations were then sorted by flow cytometry, cytospun, and immunolabeled for Sox2.

All GFP + cells coexpressed Sox2, whereas GFP− cells did not express Sox2 (Fig. 8D). *eGFP* + cells from β-actin-GFP/ + mice were used as a positive control.

Discussion

The present study characterized the heterogeneous cells that accumulate at the site of injury in response to treatment with ECM degradation products in an adult mammalian model of digit amputation. In addition to periosteal localization and coexpression of mesenchymal stem cell markers Sca1 and CD90, the present study showed that the Sox2 + cells are not derived from the bone marrow or peripheral circulation.

It is surprising that chimeric studies suggest that the Sox2 + cells are not derived from bone marrow. Because the bone marrow is a source of osteoblasts, a population of cells

that has recently been shown to require Sox2 expression for self-renewal,[30] it would be expected that at least a subset of the Sox2+ cells at the site of digit amputation involving bone injury would be derived from the bone marrow. However, it is unclear whether Sox2 is only transiently expressed in osteoblasts, or only expressed in a small subset of osteoblasts. Furthermore, previous studies have shown that osteoblasts alter their phenotype *in vitro* upon constitutive expression of Sox2.[31] Thus, it is possible that osteoblasts in a normal homeostatic situation do not constitutively express Sox2. A more likely explanation for the findings of the present study is that the Sox2+ cells at the site of amputation are derived from the injured periosteum surrounding the amputated bone. The periosteum is a known source of osteogenic precursors, including osteoblasts,[43,44] and the findings of the study suggesting a local rather than circulating source of Sox2+ cells would be consistent with a periosteal source for the Sox2+ cells.

The identification of a periosteal Sox2+ cell population at the site of injury after treatment with ECM degradation products is an unexpected finding that warrants further study. Sox2 is a transcription factor that plays an important role in the maintenance of pluripotency,[45] and it has also been found to be expressed in a restricted set of adult progenitor cells such as neural, dermal, and neural crest–derived progenitor cells.[32,33] Additionally, embryonic stem cells and neural progenitors generally show Sox2 expression restricted to the nucleus, but the present study found Sox2 expression both in the nucleus and the cytoplasm. Although the significance of cytoplasmic localization of Sox2 observed in the present study is not known, previous studies have shown that Sox2 activity can be regulated by shuttling the Sox2 transcription factor in and out of the nucleus.[46] Export of Sox2 from of the nucleus to the cytoplasm has been postulated to be an indicator of cell differentiation in Sox2+ progenitor cells.[47] Therefore, the cytoplasmic localization of Sox2 in cells may be a sign of these cells in a state of differentiation. Previous studies have also found that only a subset of Sox2+ cells at the site of amputation undergoes mitosis, consistent with the hypothesis that heterogeneity among Sox2+ cells may be due to asymmetric division and differentiation.[29]

The present study also showed that treatment with ECM degradation products results in an early increase in the number of Sox2+ cells at the site of amputation. At later time points, however, there is no difference between ECM treatment and PBS-treated control groups. The transiently increased accumulation of Sox2+ cells by ECM degradation products is most consistent with the initial phase of a non-blastemal, epimorphic regenerative response,[48,49] in which there is site-directed recruitment of cells to the site of injury. Considered in this light, the use of bioactive molecules for the site-directed accumulation of progenitor cells can be thought of as a form of endogenous stem cell therapy.[5,50] The logical next step necessary for epimorphic regeneration of tissue is to provide the accumulated cells with the proper signals and cues to proliferate and differentiate into site-appropriate, differentiated, functional tissue.

The present study has a number of limitations. The present study confirmed engraftment of Sox2 *eGFP/+* bone marrow by CD45.2+ expression in the peripheral blood of recipient wild-type CD45.1+ mice. Although GFP+ expression was confirmed in Sox2+ cells from donor mice, the present study did not confirm the presence of the Sox2:*eGFP* construct in the bone marrow of recipient mice. Additionally, the study focused on known populations of Sox2+ cells in the adult mouse as a source of the Sox2+ cells. However, the findings of the present study cannot definitively exclude the possibility that the Sox2+ cells at the site of digit amputation are more pluripotent stem cells. To this point, the present study did not determine the expression of other known pluripotency stem cell markers such as Oct-3/4 or Nanog in the Sox2+ cell population. Additionally, the present study did not directly determine the lineage differentiation potential of Sox2+ cells *in vitro* or *in vivo*. Although previous studies have shown that a subset of the cells at the site of amputation are capable of neuroectodermal and mesodermal differentiation potential *in vitro*[21] and that Sox2+ cell accumulation coincides increased bone deposition *in vivo*,[51] the differentiation potential of the Sox2+ cell population and, specifically, the contribution of the Sox2+ cell population to differentiated tissue *in vivo* are beyond the scope of the present article. Future studies will further investigate the differentiation potential of Sox2+ cells by utilizing Sox2 transgenic mouse models in which long-term tracking as well as selective manipulation of Sox2+ cells are possible.[52]

Nevertheless, the findings of the present study identified a local source of Sox2+ cells at the site of digit amputation that are increased after treatment with ECM degradation products *in vivo*. The partial characterization of a local source of Sox2+ cells adds to a growing understanding of the important mediators of the local tissue injury microenvironment that may play role in promoting constructive remodeling of the injured tissue as opposed to fibrosis. Although future work is necessary to further characterize the function and potential of the Sox2+ cells *in vivo*, the present study advances our understanding of the potential sources of cells that may need to be targeted for successful non-blastemal, epimorphic regeneration of complex tissues such as limbs and digits. Previous studies have shown that bioactive molecules, including cryptic peptides derived from enzymatic degradation of ECM proteins, can locally recruit and/or activate such cells at the site of injury. Further characterization of these recruited cells will be important for the next logical step in promoting tissue reconstruction of providing such cells with the proper signals and cues to proliferate and differentiate to functional, site-appropriate tissue.

Acknowledgments

Disclosure Statement

No competing financial interests exist.

References

1. Kumar, A., Godwin, J.W., Gates, P.B., Garza-Garcia, A.A., and Brockes, J.P. Molecular basis for the nerve dependence of limb regeneration in an adult vertebrate. Science **318,** 772, 2007.

2. Monaghan, J.R., Epp, L.G., Putta, S., Page, R.B., Walker, J.A., Beachy, C.K., *et al.* Microarray and cDNA sequence analysis of transcription during nerve-dependent limb regeneration. BMC Biol **7,** 1, 2009.

3. Kragl, M., Knapp, D., Nacu, E., Khattak, S., Maden, M., Epperlein, H.H., *et al.* Cells keep a memory of their tissue origin during axolotl limb regeneration. Nature **460,** 60, 2009.

4. Kim, J.Y., Xin, X., Moioli, E.K., Chung, J., Lee, C.H., Chen, M., *et al.* Regeneration of Dental-Pulp-like Tissue by Chemotaxis-Induced Cell Homing. Tissue Eng Part A **16,** 3023, 2010.

5. Lee, C.H., Cook, J.L., Mendelson, A., Moioli, E.K., Yao, H., and Mao, J.J. Regeneration of the articular surface of the rabbit synovial joint by cell homing: a proof of concept study. Lancet **376,** 440, 2010.

6. Caione, P., Capozza, N., Zavaglia, D., Palombaro, G., and Boldrini, R. *In vivo* bladder regeneration using small intestinal submucosa: experimental study. Pediatr Surg Int **22,** 593, 2006.

7. Cobb, M.A., Badylak, S.F., Janas, W., and Boop, F.A. Histology after dural grafting with small intestinal submucosa. Surg Neurol **46,** 389; discussion 93, 1996.

8. Lantz, G.C., Badylak, S.F., Coffey, A.C., Geddes, L.A., and Blevins, W.E. Small intestinal submucosa as a small-diameter arterial graft in the dog. J Invest Surg **3,** 217, 1990.

9. Hodde, J.P., Badylak, S.F., and Shelbourne, K.D. The Effect of Range of Motion on Remodeling of Small Intestinal Submucosa (SIS) When Used as an Achilles Tendon Repair Material in the Rabbit. Tissue Eng **3,** 27, 1997.

10. Uygun, B.E., Soto-Gutierrez, A., Yagi, H., Izamis, M.L., Guzzardi, M.A., Shulman, C., *et al.* Organ reengineering through development of a transplantable recellularized liver graft using decellularized liver matrix. Nat Med **16,** 814, 2010.

11. Ott, H.C., Clippinger, B., Conrad, C., Schuetz, C., Pomerantseva, I., Ikonomou, L., *et al.* Regeneration and orthotopic transplantation of a bioartificial lung. Nat Med **16,** 927, 2010.

12. Ott, H.C., Matthiesen, T.S., Goh, S.K., Black, L.D., Kren, S.M., Netoff, T.I., *et al.* Perfusion-decellularized matrix: using nature's platform to engineer a bioartificial heart. Nat Med **14,** 213, 2008.

13. Badylak, S., Meurling, S., Chen, M., and Spievack, A., Simmons-Byrd A. Resorbable bioscaffold for esophageal repair in a dog model. J Pediatr Surg **35,** 1097, 2000.

14. Metcalf, M.H., Savoie, F.H., and Kellum, B. Surgical technique for xenograft (SIS) augmentation of rotator-cuff repairs. Oper Tech Orthop **12,** 204, 2002.

15. Derwin, K.A., Badylak, S.F., Steinmann, S.P., and Iannotti, J.P. Extracellular matrix scaffold devices for rotator cuff repair. J Shoulder Elbow Surg **19,** 467, 2010.

16. Mase, V.J., Jr., Hsu, J.R., Wolf, S.E., Wenke, J.C., Baer, D.G., Owens, J., *et al.* Clinical application of an acellular biologic scaffold for surgical repair of a large, traumatic quadriceps femoris muscle defect. Orthopedics **33,** 511, 2010.

17. Witteman, B.P., Foxwell, T.J., Monsheimer, S., Gelrud, A., Eid, G.M., Nieponice, A., *et al.* Transoral endoscopic inner layer esophagectomy: management of high-grade dysplasia and superficial cancer with organ preservation. J Gastrointest Surg **13,** 2104, 2009.

18. Badylak, S.F., Hoppo, T., Nieponice, A., Gilbert, T.W., Davison, J.M., and Jobe, B.A. Esophageal preservation in five male patients after endoscopic inner-layer circumferential resection in the setting of superficial cancer: a regenerative medicine approach with a biologic scaffold. Tissue Eng Part A **17,** 1643, 2011.

19. Zantop, T., Gilbert, T.W., Yoder, M.C., and Badylak, S.F. Extracellular matrix scaffolds are repopulated by bone marrow-derived cells in a mouse model of achilles tendon reconstruction. J Orthop Res **24,** 1299, 2006.

20. Badylak, S.F., Park, K., Peppas, N., McCabe, G., and Yoder, M. Marrow-derived cells populate scaffolds composed of xenogeneic extracellular matrix. Exp Hematol **29,** 1310, 2001.

21. Agrawal, V., Johnson, S.A., Reing, J., Zhang, L., Tottey, S., Wang, G., *et al.* Epimorphic regeneration approach to tissue replacement in adult mammals. Proc Natl Acad Sci U S A **107,** 3351, 2010.

22. Valentin, J.E., Stewart-Akers, A.M., Gilbert, T.W., and Badylak, S.F. Macrophage participation in the degradation and remodeling of extracellular matrix scaffolds. Tissue Eng Part A **15,** 1687, 2009.

23. Badylak, S.F., Valentin, J.E., Ravindra, A.K., McCabe, G.P., and Stewart-Akers, A.M. Macrophage phenotype as a determinant of biologic scaffold remodeling. Tissue Eng Part A **14,** 1835, 2008.

24. Valentin, J.E., Badylak, J.S., McCabe, G.P., and Badylak, S.F. Extracellular matrix bioscaffolds for orthopaedic applications. A comparative histologic study. J Bone Joint Surg Am **88,** 2673, 2006.

25. Reing, J.E., Zhang, L., Myers-Irvin, J., Cordero, K.E., Freytes, D.O., Heber-Katz, E., *et al.* Degradation products of extracellular matrix affect cell migration and proliferation. Tissue Eng Part A **15,** 605, 2009.

26. Brennan, E.P., Tang, X.H., Stewart-Akers, A.M., Gudas, L.J., and Badylak, S.F. Chemoattractant activity of degradation products of fetal and adult skin extracellular matrix for keratinocyte progenitor cells. J Tissue Eng Regen Med **2,** 491, 2008.

27. Crisan, M., Yap, S., Casteilla, L., Chen, C.W., Corselli, M., Park, T.S., *et al.* A perivascular origin for mesenchymal stem cells in multiple human organs. Cell Stem Cell **3,** 301, 2008.

28. Agrawal, V., Siu, B.F., Chao, H., Hirschi, K.K., Raborn, E., Johnson, S.A., *et al.* An isolated cryptic peptide influences osteogenesis and bone remodeling in an adult mammalian model of digit amputation. Tissue Eng Part A **17,** 3033, 2011.

29. Agrawal, V., Tottey, S., Johnson, S.A., Freund, J., Siu, B.F., and Badylak, S.F. Recruitment of progenitor cells by an ecm cryptic peptide in a mouse model of digit amputation. Tissue Eng Part A **17,** 2435, 2011.

30. Basu-Roy, U., Ambrosetti, D., Favaro, R., Nicolis, S.K., Mansukhani, A., and Basilico, C. The transcription factor Sox2 is required for osteoblast self-renewal. Cell Death Differ **17,** 1345, 2011.

31. Mansukhani, A., Ambrosetti, D., Holmes, G., Cornivelli, L., and Basilico, C. Sox2 induction by FGF and FGFR2 activating mutations inhibits Wnt signaling and osteoblast differentiation. J Cell Biol **168,** 1065, 2005.

32. Hutton, S.R., and Pevny, L.H. SOX2 expression levels distinguish between neural progenitor populations of the developing dorsal telencephalon. Dev Biol **352,** 40, 2011.

33. Biernaskie, J., Paris, M., Morozova, O., Fagan, B.M., Marra, M., Pevny, L., *et al.* SKPs derive from hair follicle precursors and exhibit properties of adult dermal stem cells. Cell Stem Cell **5,** 610, 2009.

34. Freytes, D.O., Badylak, S.F., Webster, T.J., Geddes, L.A., and Rundell, A.E. Biaxial strength of multilaminated extracellular matrix scaffolds. Biomaterials **25,** 2353, 2004.

35. Mirzadeh, Z., Merkle, F.T., Soriano-Navarro, M., Garcia-Verdugo, J.M., and Alvarez-Buylla, A. Neural stem cells confer unique pinwheel architecture to the ventricular surface in neurogenic regions of the adult brain. Cell Stem Cell **3,** 265, 2008.

36. Ellis, P., Fagan, B.M., Magness, S.T., Hutton, S., Taranova, O., Hayashi. S., *et al.* SOX2, a persistent marker for multipotential neural stem cells derived from embryonic stem cells, the embryo or the adult. Dev Neurosci **26,** 148, 2004.

37. Tavazoie, M., Van der Veken, L., Silva-Vargas, V., Louissaint, M., Colonna, L., Zaidi, B., *et al.* A specialized vascular niche for adult neural stem cells. Cell Stem Cell **3,** 279, 2008.

38. Christensen, P.J., Goodman, R.E., Pastoriza, L., Moore, B., and Toews, G.B. Induction of lung fibrosis in the mouse by intratracheal instillation of fluorescein isothiocyanate is not T-cell-dependent. Am J Pathol **155,** 1773, 1999.

39. Schotte, O.E., and Smith, C.B. Wound Healing Processes in Amputated Mouse Digits. Biological Bulletin **117,** 546, 1959.

40. Schotte, O.E., and Smith, C.B. Effects of ACTH and of cortisone upon amputational wound healing processes in mice digits. J Exp Zool **146,** 209, 1961.

41. Spangrude, G.J., Heimfeld, S., and Weissman, I.L. Purification and characterization of mouse hematopoietic stem cells. Science **241,** 58, 1988.

42. Spangrude, G.J., and Scollay, R. A simplified method for enrichment of mouse hematopoietic stem cells. Exp Hematol **18,** 920, 1990.

43. De Bari, C., Dell'Accio, F., Vanlauwe, J., Eyckmans, J., Khan, I.M., Archer, C.W., *et al.* Mesenchymal multipotency of adult human periosteal cells demonstrated by single-cell lineage analysis. Arthritis Rheum **54,** 1209, 2006.

44. Zhang, X., Xie, C., Lin, A.S., Ito, H., Awad, H., Lieberman, J.R., *et al.* Periosteal progenitor cell fate in segmental cortical bone graft transplantations: implications for functional tissue engineering. J Bone Miner Res **20,** 2124, 2005.

45. Avilion, A.A., Nicolis, S.K., Pevny, L.H., Perez, L., Vivian, N., and Lovell-Badge, R. Multipotent cell lineages in early mouse development depend on SOX2 function. Genes Dev **17,** 126, 2003.

46. Baltus, G.A., Kowalski, M.P., Zhai, H., Tutter, A.V., Quinn, D., Wall, D., *et al.* Acetylation of sox2 induces its nuclear export in embryonic stem cells. Stem Cells **27,** 2175, 2009.

47. Li, J., Pan, G., Cui, K., Liu, Y., Xu, S., and Pei, D. A dominant-negative form of mouse SOX2 induces trophectoderm differentiation and progressive polyploidy in mouse embryonic stem cells. J Biol Chem **282,** 19481, 2007.

48. Morgan, T.H. Regeneration. New York, NY: Macmillan & Co., Ltd., 1901.

49. Sanchez Alvarado, A. Regeneration in the metazoans: why does it happen? Bioessays **22,** 578, 2000.

50. Kim, J.Y., Xin, X., Moioli, E.K., Chung, J., Lee, C.H., Chen, M., *et al.* Regeneration of dental-pulp-like tissue by chemotaxis-induced cell homing. Tissue Eng Part A **16,** 3023, 2010.

51. Agrawal, V., Kelly, J., Tottey, S., Daly, K.A., Johnson, S.A., Siu, B.F., *et al.* An isolated cryptic Peptide influences osteogenesis and bone remodeling in an adult Mammalian model of digit amputation. Tissue Eng Part A **17,** 3033, 2011.

52. Favaro, R., Valotta, M., Ferri, A.L., Latorre, E., Mariani, J., Giachino, C., *et al.* Hippocampal development and neural stem cell maintenance require Sox2-dependent regulation of Shh. Nat Neurosci **12,** 1248, 2009.

Address correspondence to:
Stephen F. Badylak, D.V.M., M.D., Ph.D.
McGowan Institute for Regenerative Medicine
Bridgeside Point II Building
University of Pittsburgh
450 Technology Drive, Suite 300
Pittsburgh, PA 15213

E-mail: badylaks@upmc.edu